

Supplementary Information for

Redox-Mediator Enhanced Electrochemiluminescence under Non-Aqueous Conditions

Steven J. Blom,^{a,†} Fazeleh Mesgari,^{a,†} El M. S. Martin,^a Egan H. Doeven,^a David J. Hayne,^b Timothy U. Connell,^a Peter J. Barnard,^c Narges Saeedizadeh,^d Seyed Mohammad Jafar Jalali,^e Paul S. Francis^{a,*}

^aCentre for Sustainable Bioproducts, Faculty of Science, Engineering and Built Environment, Deakin University, Geelong, Victoria 3220, Australia.

^bInstitute for Frontier Materials, Faculty of Science, Engineering and Built Environment, Deakin University, Geelong, Victoria 3220, Australia.

^cDepartment of Biochemistry and Chemistry, La Trobe Institute for Molecular Science, La Trobe University, Victoria 3086, Australia.

^dInstitute for Intelligent Systems Research and Innovation, Deakin University, Geelong, Victoria 3220, Australia.

^eSchool of Science, Edith Cowan University, Joondalup, Western Australia 6027, Australia.

[†]These authors contributed equally.

*Author for correspondence.

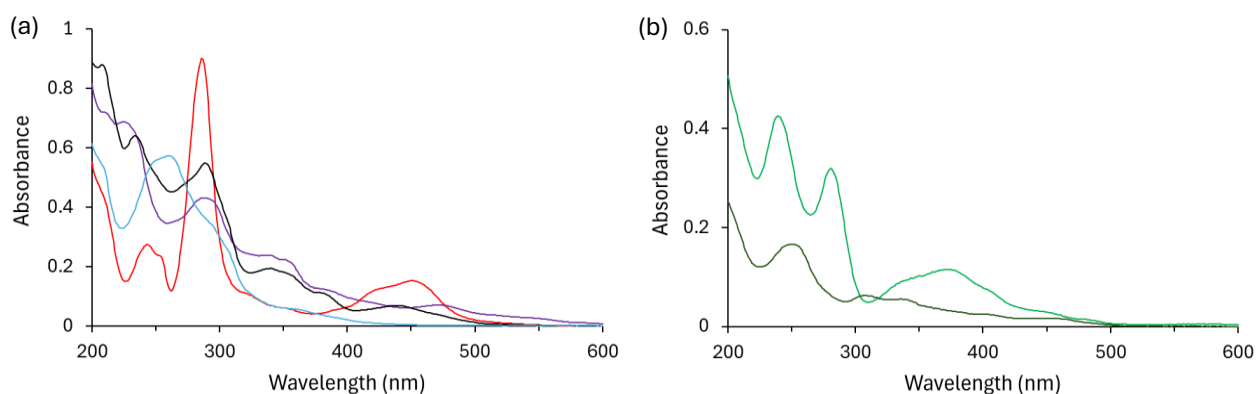


Figure S1. UV-Vis absorption spectra of (a) luminophores: $[\text{Ru}(\text{bpy})_3]^{2+}$ (red trace), $[\text{Ir}(\text{piq})_2(\text{dm-bpy})]^+$ (black trace), $\text{Ir}(\text{piq})_2(\text{acac})$ (purple trace), and $[\text{Ir}(\text{df-ppy})_2(\text{dm-bpy})]^+$ (blue trace); and (b) redox mediators: $\text{Ir}(\text{ppy})_3$ (light green trace) and $\text{Ir}(\text{ppy})_2(\text{acac})$ (dark green trace). Conditions: $10 \mu\text{M}$ metal complex in acetonitrile at ambient temperature.

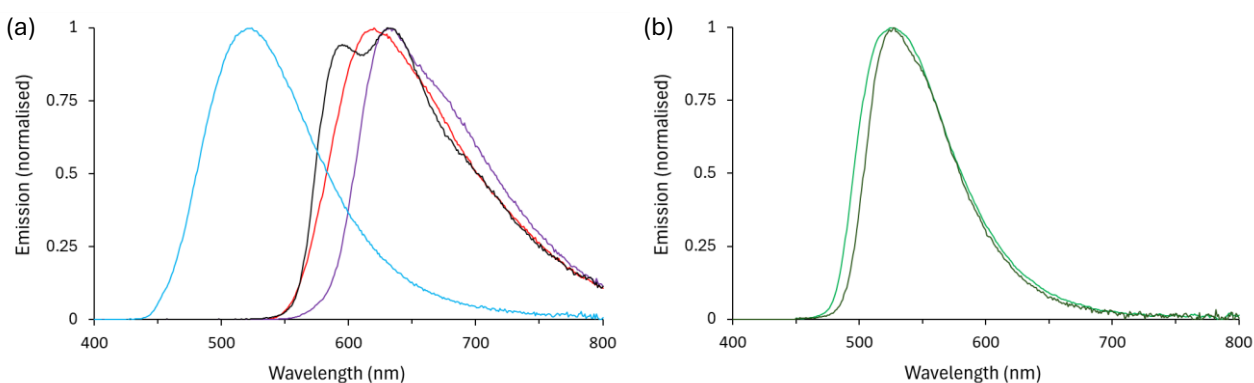


Figure S2. Photoluminescence emission spectra of (a) luminophores: $[\text{Ru}(\text{bpy})_3]^{2+}$ (red trace), $[\text{Ir}(\text{piq})_2(\text{dm-bpy})]^+$ (black trace), $\text{Ir}(\text{piq})_2(\text{acac})$ (purple trace), and $[\text{Ir}(\text{df-ppy})_2(\text{dm-bpy})]^+$ (blue trace); and (b) redox mediators: $\text{Ir}(\text{ppy})_3$ (light green trace) and $\text{Ir}(\text{ppy})_2(\text{acac})$ (dark green trace). Conditions: $10 \mu\text{M}$ metal complex in acetonitrile at ambient temperature.

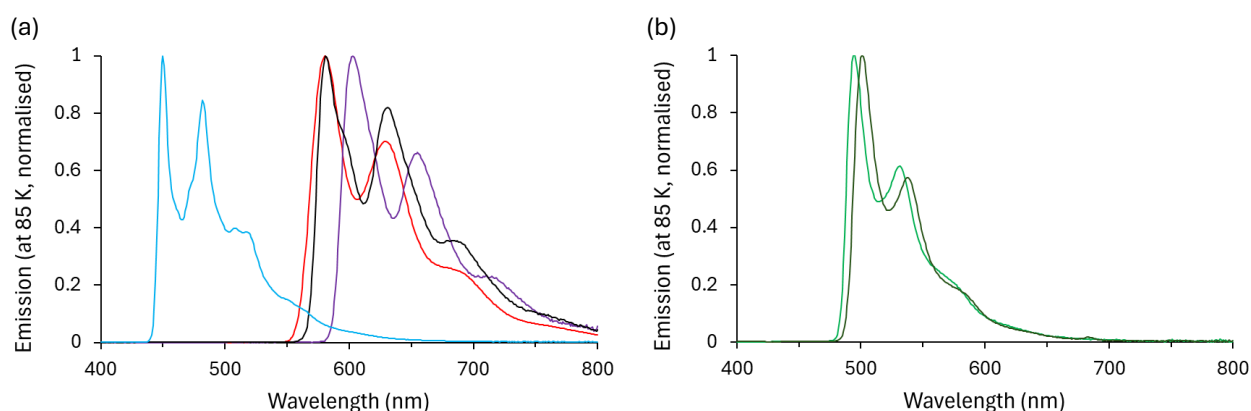


Figure S3. Low temperature photoluminescence emission spectra of (a) luminophores: $[\text{Ru}(\text{bpy})_3]^{2+}$ (red trace), $[\text{Ir}(\text{piq})_2(\text{dm-bpy})]^+$ (black trace), $\text{Ir}(\text{piq})_2(\text{acac})$ (purple trace), and $[\text{Ir}(\text{df-ppy})_2(\text{dm-bpy})]^+$ (blue trace); and (b) redox mediators: $\text{Ir}(\text{ppy})_3$ (light green trace) and $\text{Ir}(\text{ppy})_2(\text{acac})$ (dark green trace). Conditions: $5 \mu\text{M}$ metal complex in 4:1 spectrometric grade EtOH/MeOH at 85 K.

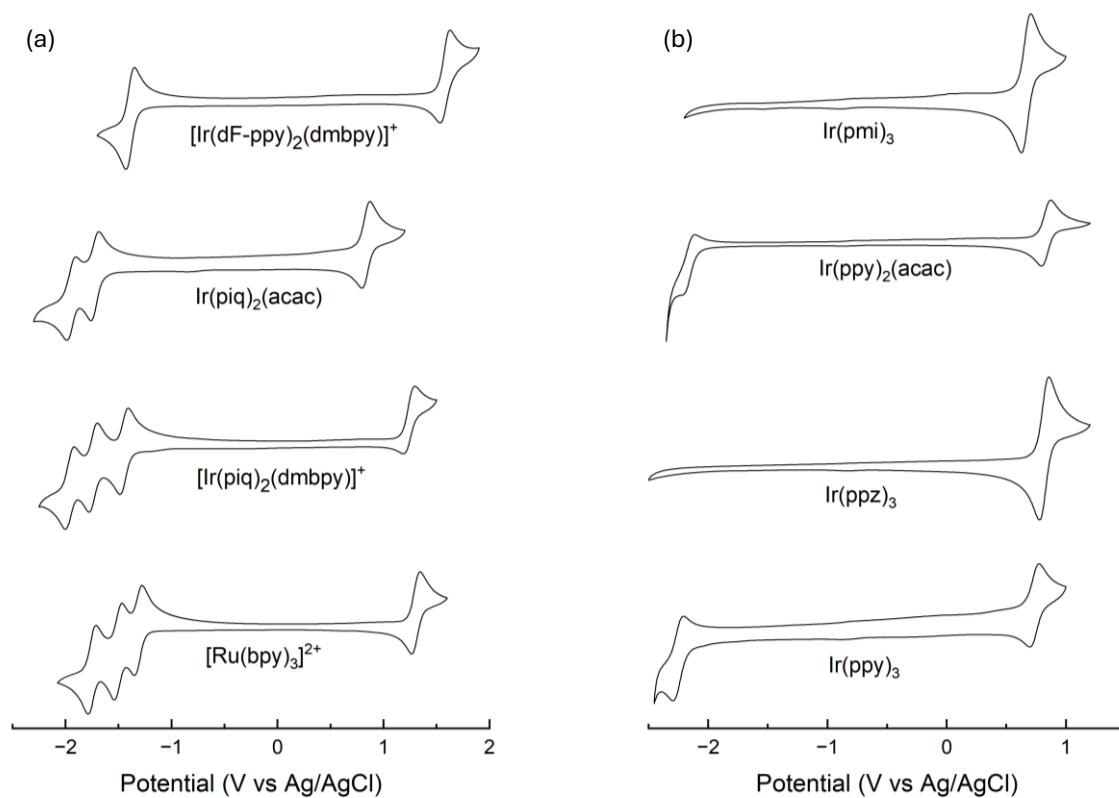


Figure S4. Cyclic voltammograms of (a) luminophores: $[\text{Ru}(\text{bpy})_3]^{2+}$, $[\text{Ir}(\text{piq})_2(\text{dm-bpy})]^+$, $\text{Ir}(\text{piq})_2(\text{acac})$, and $[\text{Ir}(\text{df-ppy})_2(\text{dm-bpy})]^+$; and (b) redox mediators: $\text{Ir}(\text{ppy})_3$, $\text{Ir}(\text{ppz})_3$, $\text{Ir}(\text{ppy})_2(\text{acac})$, and $\text{Ir}(\text{pmi})_3$. Conditions: 1 mM metal complex (except for $\text{Ir}(\text{ppy})_3$ (0.2 mM), $\text{Ir}(\text{piq})_2(\text{acac})$ (0.5 mM) and $\text{Ir}(\text{ppy})_2(\text{acac})$ (0.5 mM) in acetonitrile with 0.1 M TBAPF_6 as supporting electrolyte.

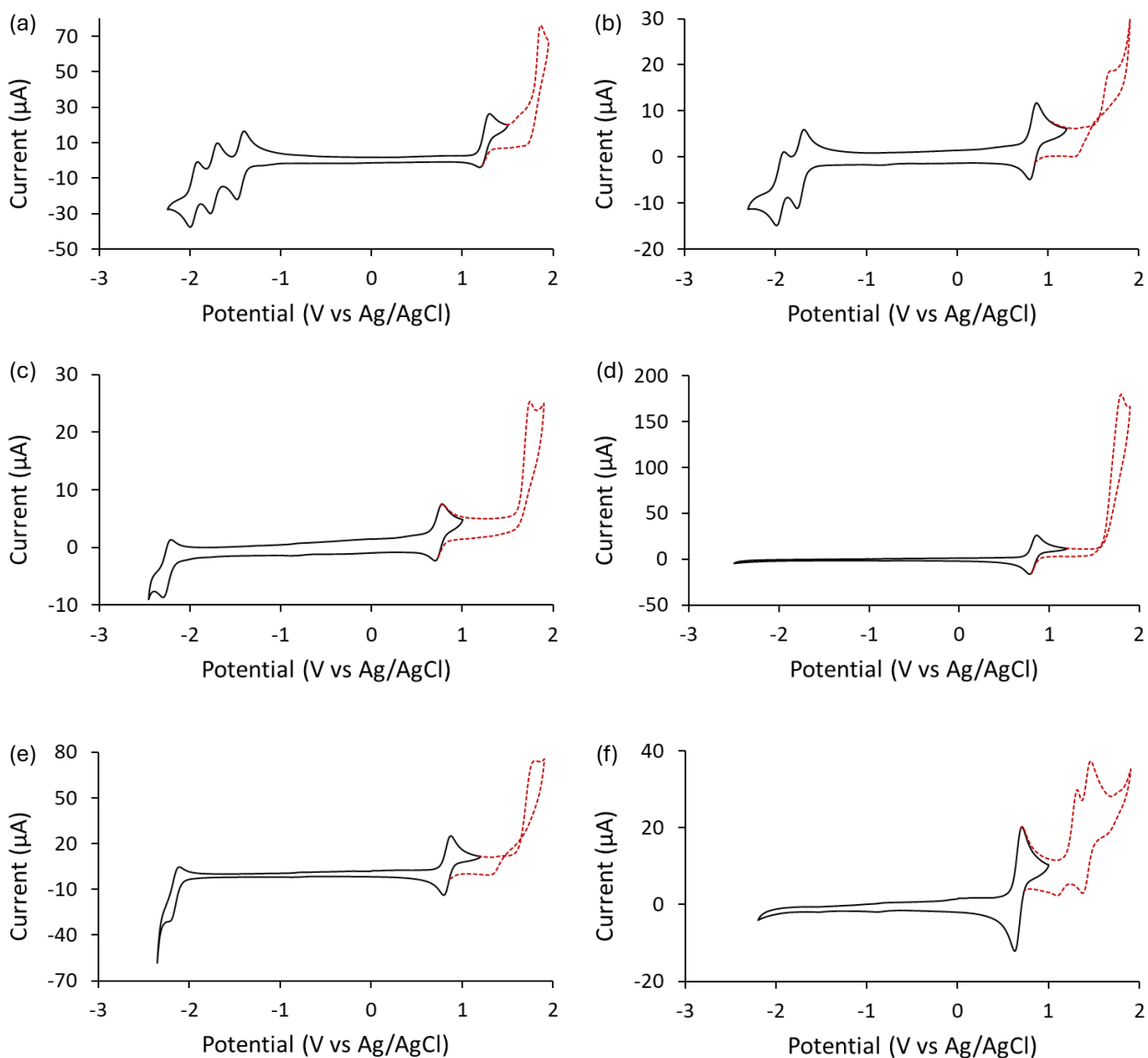


Figure S5. Cyclic voltammograms showing subsequent oxidation of (a) 1 mM [Ir(piq)₂(dm-bpy)]⁺, (b) 0.5 mM Ir(piq)₂(acac), (c) 0.2 mM Ir(ppy)₃, (d) 1 mM Ir(ppz)₃, (e) 1 mM Ir(ppy)₂(acac), and (f) 1 mM Ir(pmi)₃, in acetonitrile with 0.1 M TBAPF₆ as supporting electrolyte.

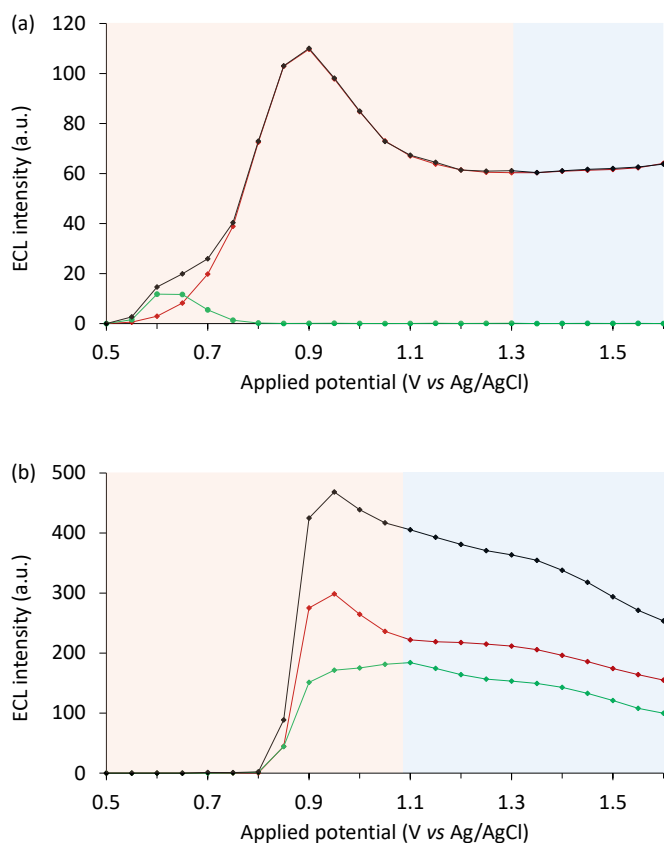


Figure S6. (a) Combined ECL intensity (integrated spectral distribution) of a mixture of $10 \mu\text{M}$ $[\text{Ru}(\text{bpy})_3]^{2+}$ and $100 \mu\text{M}$ $\text{Ir}(\text{ppy})_3$ at different applied potentials in acetonitrile with 10 mM TPrA and 0.1 M TBAPF₆ (black plot), and the deconvoluted contributions from $[\text{Ru}(\text{bpy})_3]^{2+}$ (red plot) and $\text{Ir}(\text{ppy})_3$ (green plot), as shown in Fig. S7. (b) Combined ECL intensity (integrated spectral distribution) of a mixture of $1 \mu\text{M}$ $[\text{Ru}(\text{bpy})_3]^{2+}$ and $100 \mu\text{M}$ $[\text{Ir}(\text{sppy})_3]^{3-}$ at different applied potentials in aqueous ProCell buffer containing 180 mM TPrA (black plot), and the deconvoluted contributions from $[\text{Ru}(\text{bpy})_3]^{2+}$ (red plot) and $[\text{Ir}(\text{sppy})_3]^{3-}$ (green plot).

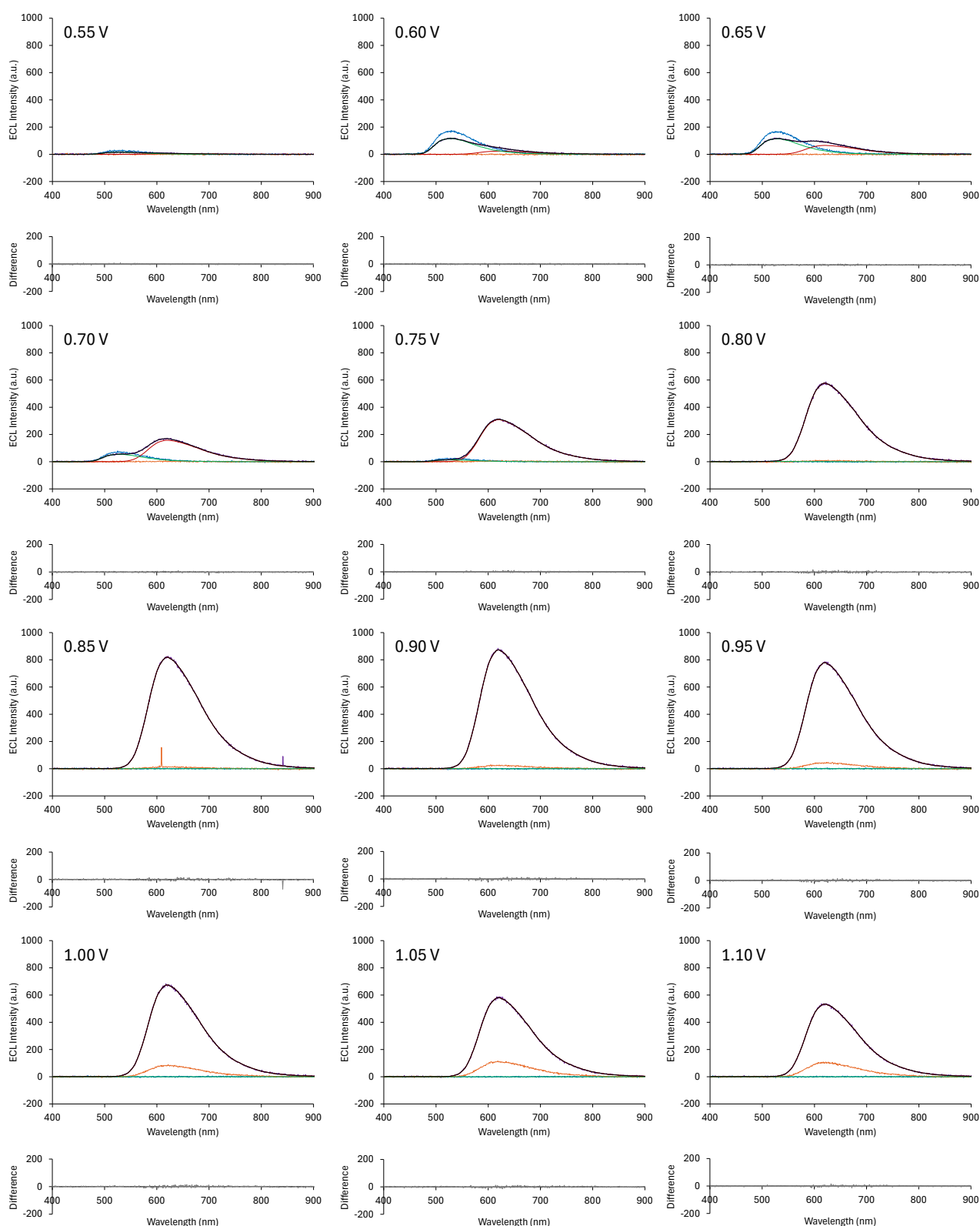


Figure S7. Selected spectra obtained from spooling ECL experiments for the [Ru(bpy)₃]²⁺ luminophore (orange plot), Ir(ppy)₃ mediator (blue plot), and a mixture of [Ru(bpy)₃]²⁺ and Ir(ppy)₃ (purple plot). The black plot shows the model spectrum of the mixture, which was deconvoluted into contributions from [Ru(bpy)₃]²⁺ (red plot) and Ir(ppy)₃ (green plot). The residuals for the modelled ECL spectrum are shown in the grey plot below. Experimental conditions: 10 μM luminophore and/or 100 μM redox mediator in acetonitrile containing 10 mM TPrA as co-reactant and 0.1 M TBAPF₆ as supporting electrolyte.

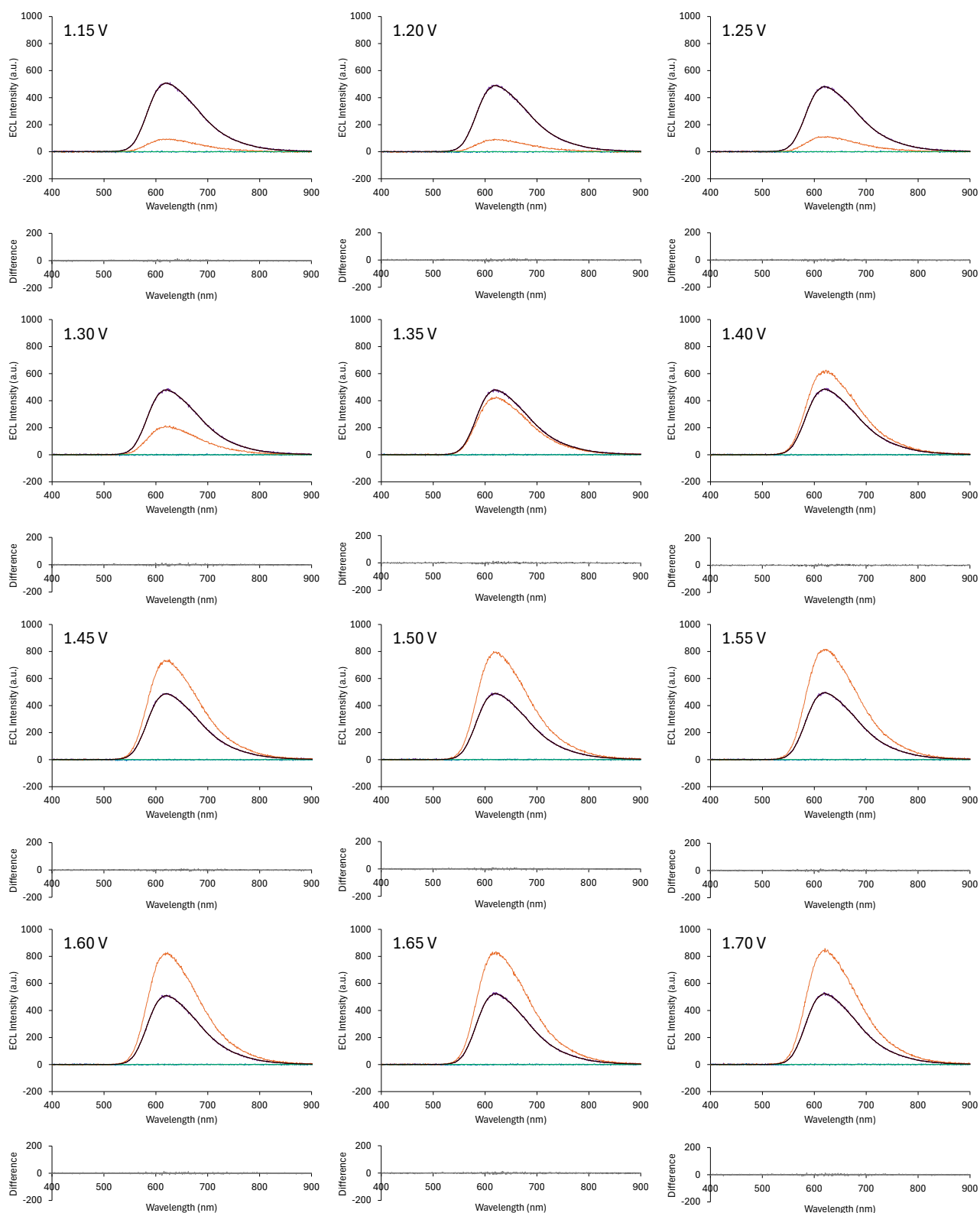


Figure S7 (continued). Selected spectra obtained from spooling ECL experiments for the [Ru(bpy)₃]²⁺ luminophore (orange plot), Ir(ppy)₃ mediator (blue plot), and a mixture of [Ru(bpy)₃]²⁺ and Ir(ppy)₃ (purple plot). The black plot shows the model spectrum of the mixture, which was deconvoluted into contributions from [Ru(bpy)₃]²⁺ (red plot) and Ir(ppy)₃ (green plot). The residuals for the modelled ECL spectrum are shown in the grey plot below. Experimental conditions: 10 μM luminophore and/or 100 μM redox mediator in acetonitrile containing 10 mM TPrA as co-reactant and 0.1 M TBAPF₆ as supporting electrolyte.

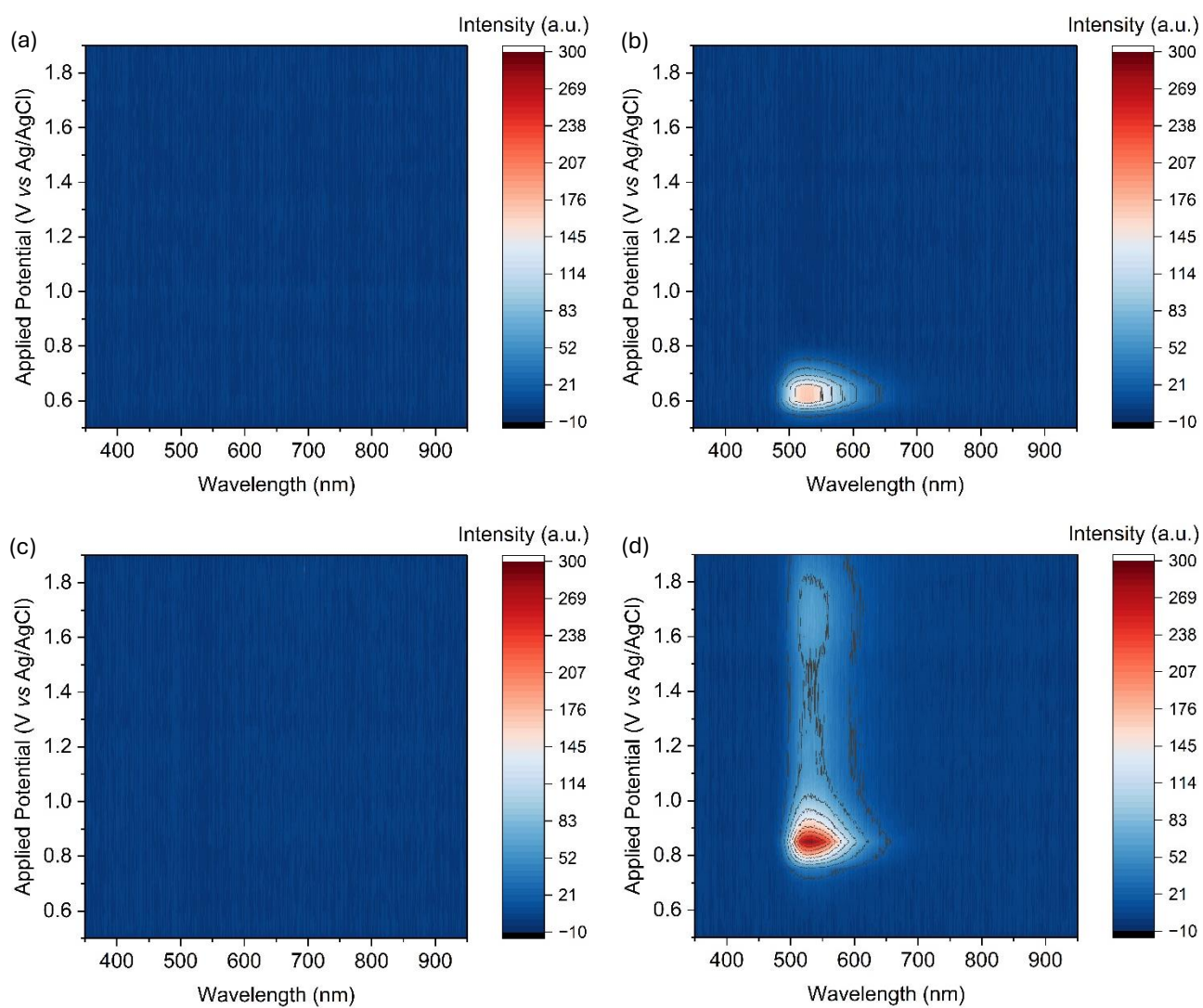


Figure S8. Contour plots of ECL intensity versus wavelength and applied potential for the redox mediators: (a) $\text{Ir}(\text{pmi})_3$, (b) $\text{Ir}(\text{ppy})_3$, (c) $\text{Ir}(\text{ppz})_3$, or (d) $\text{Ir}(\text{ppy})_2(\text{acac})$. Conditions: 100 μM redox mediator in acetonitrile containing 10 mM TPrA as co-reactant and 0.1 M TBAPF_6 as supporting electrolyte.

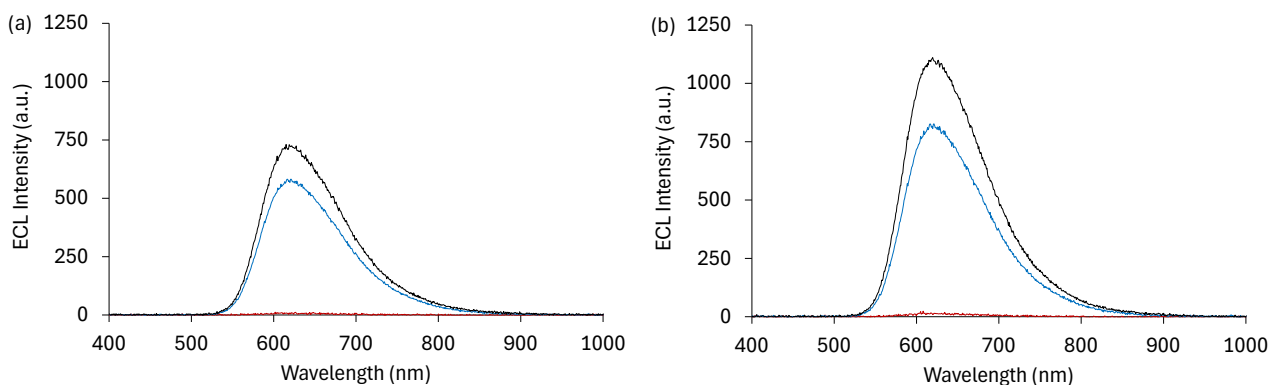


Figure S9. Co-reactant ECL spectrum of $[\text{Ru}(\text{bpy})_3]^{2+}$ ($10 \mu\text{M}$) at (a) 0.80 V and (b) 0.85 V vs Ag/AgCl , without a redox mediator (red plots), with $\text{Ir}(\text{ppy})_3$ ($100 \mu\text{M}$, blue plots), or with $\text{Ir}(\text{ppz})_3$ ($100 \mu\text{M}$, black plots). Data extracted from that shown in Fig. 3b and 3c, respectively. Where required, the emission from $[\text{Ru}(\text{bpy})_3]^{2+}$ was deconvoluted from that of $\text{Ir}(\text{ppy})_3$ (Fig. S6, S7). At 0.80 V and 0.85 V , the ECL intensity of $[\text{Ru}(\text{bpy})_3]^{2+}$ was increased by 125- and 71-fold by $\text{Ir}(\text{ppy})_3$ and 157- and 96-fold by $\text{Ir}(\text{ppz})_3$, respectively.

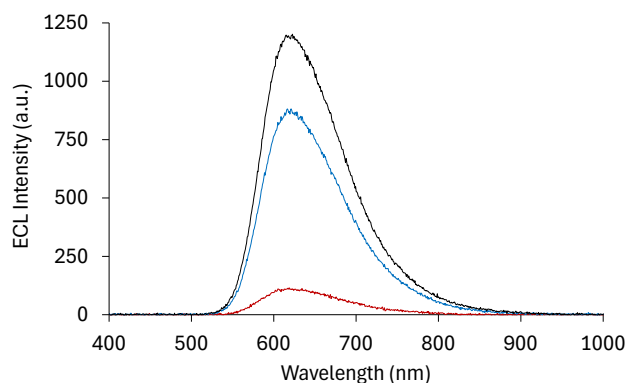


Figure S10. Co-reactant ECL spectrum of $[\text{Ru}(\text{bpy})_3]^{2+}$ ($10 \mu\text{M}$) without a redox mediator at 1.05 V vs Ag/AgCl , (red plot), with $\text{Ir}(\text{ppy})_3$ ($100 \mu\text{M}$) at 0.90 V vs Ag/AgCl (blue plot), or with $\text{Ir}(\text{ppz})_3$ ($100 \mu\text{M}$) at 0.90 V vs Ag/AgCl (black plot). Data extracted from that shown in Fig. 3b and 3c, respectively. Where required, the emission from $[\text{Ru}(\text{bpy})_3]^{2+}$ was deconvoluted from that of $\text{Ir}(\text{ppy})_3$ (Fig. S6, S7). Compared to the maximum intensity of the unenhanced first wave (at 1.05 V), the addition of $\text{Ir}(\text{ppy})_3$ and $\text{Ir}(\text{ppz})_3$ increased the ECL intensity (measured at 0.90 V vs Ag/AgCl) by 8.2- and 11-fold, respectively.

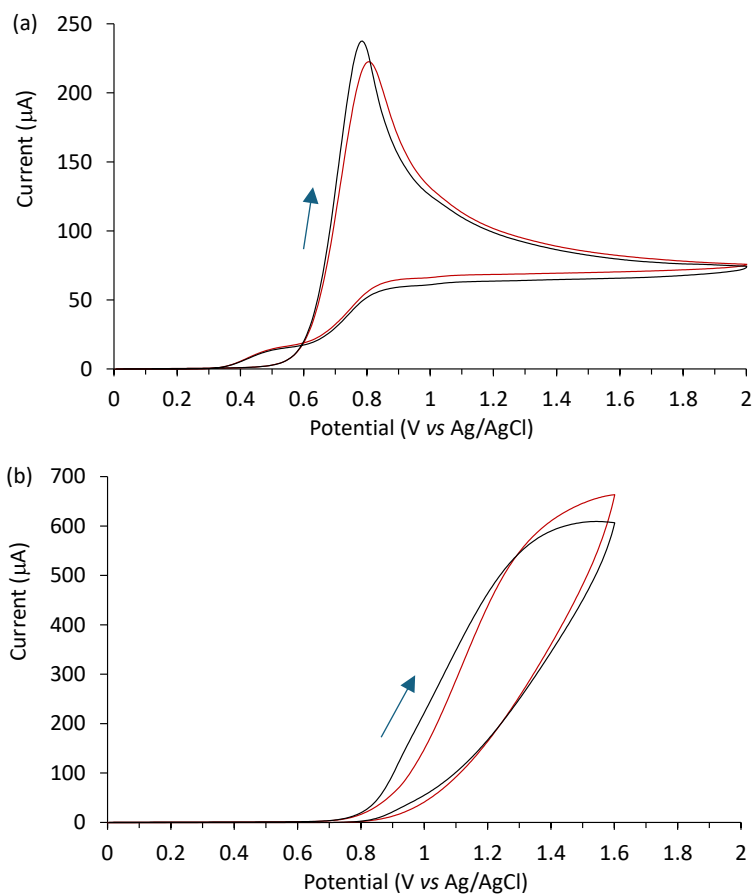


Figure S11. Cyclic voltammograms of: (a) 10 mM TPrA in ACN with 0.1 TBAPF₆ without a redox mediator (red plot) or with 200 μM Ir(ppz)₃ (black plot); and (b) aqueous ProCell solution containing 180 mM TPrA, 0.1% polidocanol, 0.3 M phosphate buffer, pH 6.8 without a redox mediator (red plot) or with 200 μM [Ir(sppz)₃]³⁻ (black plot). Data for Fig. S11b is from Adamson *et al.*, *Angew. Chem. Int. Ed.*, 2024, 63, e202412097. Scan rate 0.1 V s⁻¹. The arrows show the forward scan.

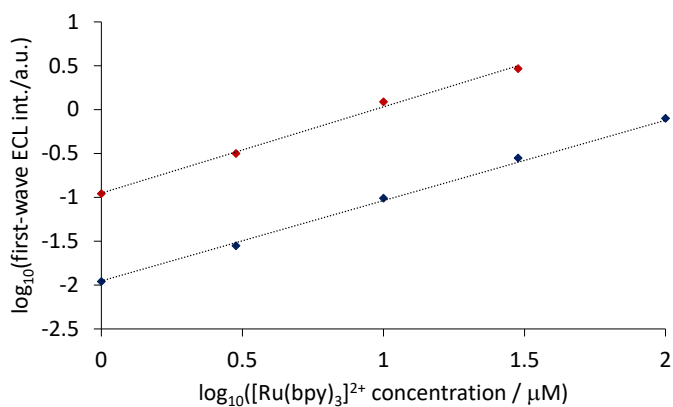


Figure S12. Log-log plot of first-wave ECL intensity versus $[\text{Ru}(\text{bpy})_3]^{2+}$ concentration, with no redox mediator (blue plot) or 100 μM $\text{Ir}(\text{ppz})_3$ (red plot). Data from Fig. 4c.

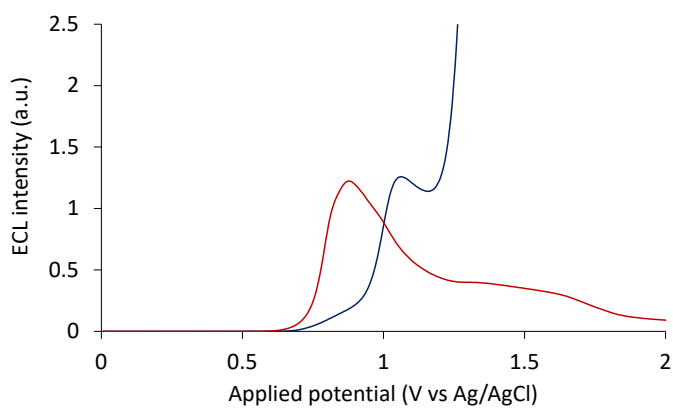


Figure S13. ECL intensity measured while scanning the applied potential from 0 to 2 V vs Ag/AgCl, using 10 μM $[\text{Ru}(\text{bpy})_3]^{2+}$ and 100 μM $\text{Ir}(\text{ppz})_3$ (red plot), or 200 μM $[\text{Ru}(\text{bpy})_3]^{2+}$ with no redox mediator (blue plot). Conditions: 10 mM TPrA in acetonitrile with 0.1 M TBAPF₆ as supporting electrolyte.

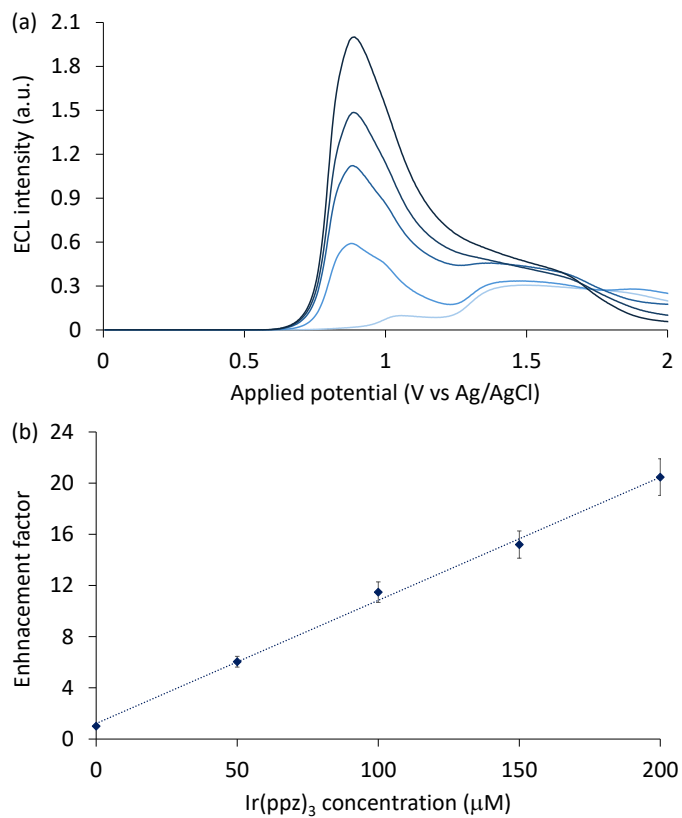


Figure S14. (a) ECL intensity measured while scanning the applied potential from 0 to 2 V vs Ag/AgCl, and (b) Enhancement of the first-wave ECL, using 10 μM [Ru(bpy)₃]²⁺ with 0, 50, 100, 150, and 200 μM Ir(ppz)₃. Conditions: 10 mM TPrA in acetonitrile with 0.1 M TBAPF₆ as supporting electrolyte.

=

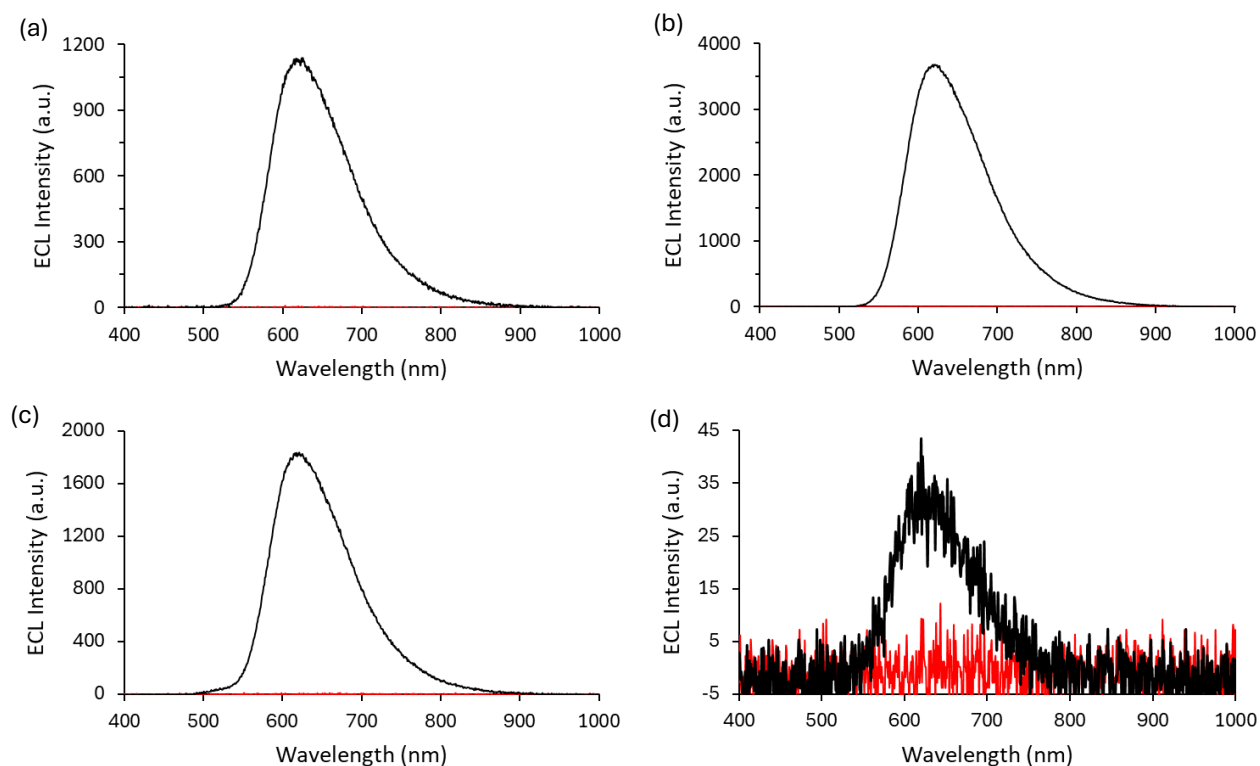


Figure S15. Mixed annihilation spectra (black plots) of a mixture of $[\text{Ru}(\text{bpy})_3]^{2+}$ ($10 \mu\text{M}$) and (a) $\text{Ir}(\text{ppy})_3$, (b) $\text{Ir}(\text{ppz})_3$, (c) $\text{Ir}(\text{ppy})_2(\text{acac})$, or (d) $\text{Ir}(\text{pmi})_3$ ($100 \mu\text{M}$), collected by alternating the applied potential (2.5 Hz for 2 s) between -1.40 V vs Ag/AgCl (to reduce $[\text{Ru}(\text{bpy})_3]^{2+}$) and 0.10 V beyond the E_{ox} of the redox mediator. The red plots show the spectra collected when applying the same potential pulse sequence in the absence of the redox mediator.

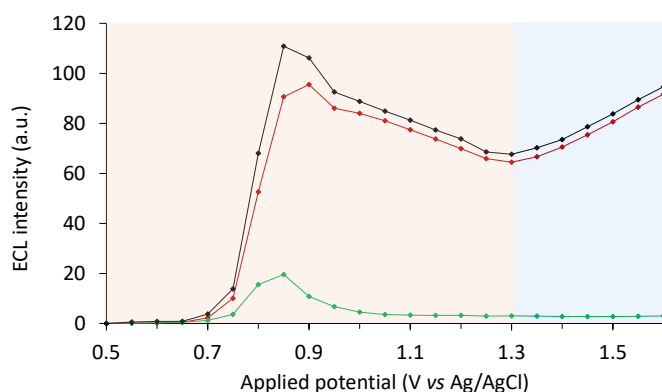


Figure S16. Combined ECL intensity (integrated spectral distribution) of a mixture of $10 \mu\text{M}$ $[\text{Ru}(\text{bpy})_3]^{2+}$ and $100 \mu\text{M}$ $\text{Ir}(\text{ppy})_2(\text{acac})$ at different applied potentials in acetonitrile with 10 mM TPrA and 0.1 M TBAPF₆ (black plot), and the deconvoluted contributions from $[\text{Ru}(\text{bpy})_3]^{2+}$ (red plot) and $\text{Ir}(\text{ppy})_2(\text{acac})$ (green plot), as shown in Fig. S17.

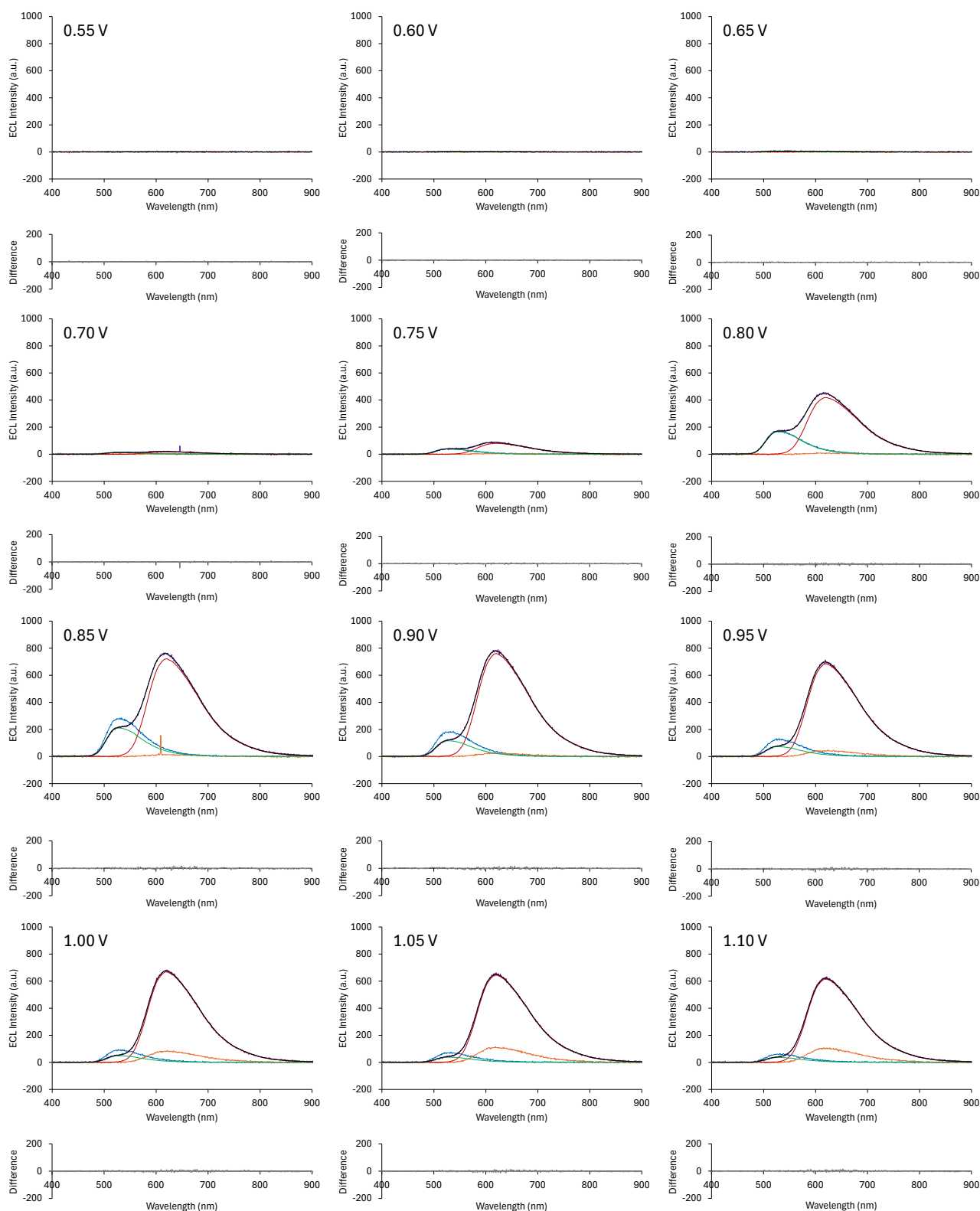


Figure S17. Selected spectra obtained from spooling ECL experiments for the $[\text{Ru}(\text{bpy})_3]^{2+}$ luminophore (orange plot), $\text{Ir}(\text{ppy})_2(\text{acac})$ mediator (blue plot), and a mixture of $[\text{Ru}(\text{bpy})_3]^{2+}$ and $\text{Ir}(\text{ppy})_2(\text{acac})$ (purple plot). The black plot shows the model spectrum of the mixture, which was deconvoluted into contributions from $[\text{Ru}(\text{bpy})_3]^{2+}$ (red plot) and $\text{Ir}(\text{ppy})_2(\text{acac})$ (green plot). The residuals for the modelled ECL spectrum are shown in the grey plot below. Experimental conditions: 10 μM luminophore and/or 100 μM redox mediator in acetonitrile containing 10 mM TPrA as co-reactant and 0.1 M TBAPF_6 as supporting electrolyte.

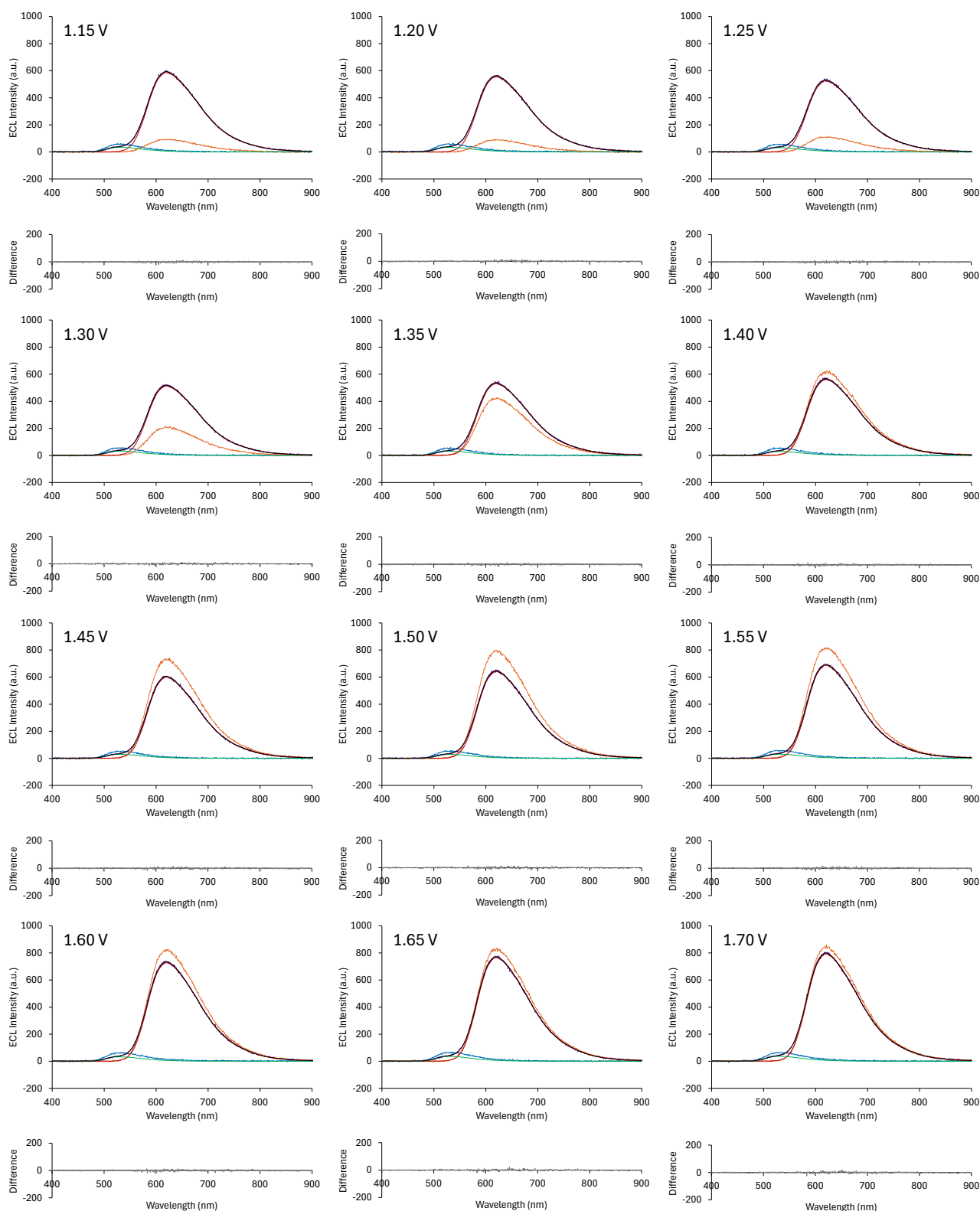


Figure S17 (continued). Selected spectra obtained from spooling ECL experiments for the $[\text{Ru}(\text{bpy})_3]^{2+}$ luminophore (orange plot), $\text{Ir}(\text{ppy})_2(\text{acac})$ mediator (blue plot), and a mixture of $[\text{Ru}(\text{bpy})_3]^{2+}$ and $\text{Ir}(\text{ppy})_2(\text{acac})$ (purple plot). The black plot shows the model spectrum of the mixture, which was deconvoluted into contributions from $[\text{Ru}(\text{bpy})_3]^{2+}$ (red plot) and $\text{Ir}(\text{ppy})_2(\text{acac})$ (green plot). The residuals for the modelled ECL spectrum are shown in the grey plot below. Experimental conditions: 10 μM luminophore and/or 100 μM redox mediator in acetonitrile containing 10 mM TPRA as co-reactant and 0.1 M TBAPF_6 as supporting electrolyte.

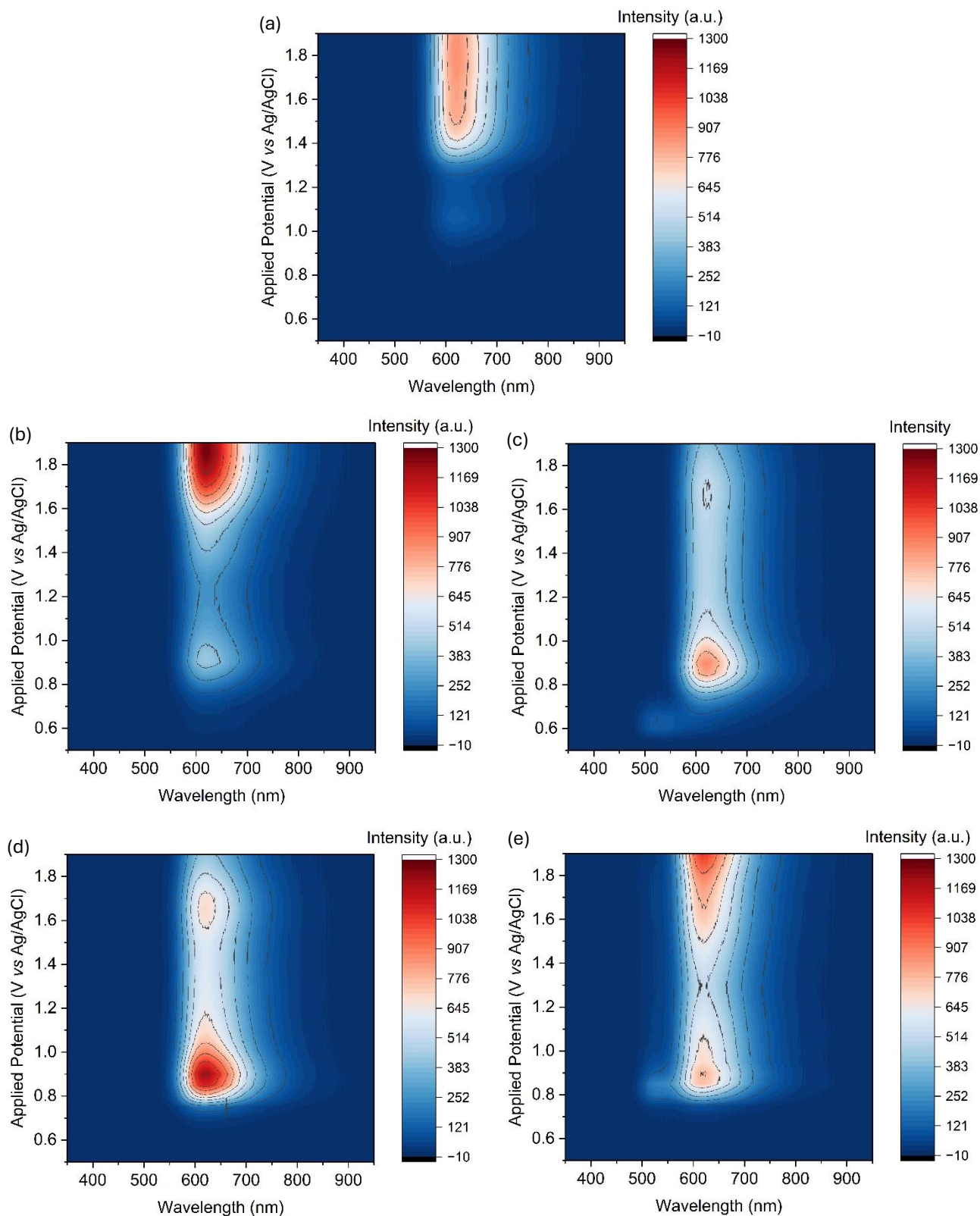


Figure S18. Contour plots of ECL intensity versus wavelength and applied potential for $[\text{Ru}(\text{bpy})_3]^{2+}$ with (a) no redox mediator, (b) $\text{Ir}(\text{pmi})_3$, (c) $\text{Ir}(\text{ppy})_3$, (d) $\text{Ir}(\text{ppz})_3$, or (e) $\text{Ir}(\text{ppy})_2(\text{acac})$. Conditions: 10 μM luminophore and 100 μM redox mediator in acetonitrile containing 10 mM TPrA as co-reactant and 0.1 M TBAPF_6 as supporting electrolyte.

To prepare each plot of ECL intensity (integrated spectrum) across the potential range from the spooling ECL approach (Fig. 3, 5, 7-9), the data from three replicate experiments was averaged before the emission from the luminophore and any emission from the redox mediator were deconvoluted, and the area under the spectrum of the luminophore at each potential was calculated. To illustrate the variation in these data, we repeated this process for the individual replicates for the $[\text{Ru}(\text{bpy})_3]^{2+}$ luminophore without enhancement, and with the four redox mediators, to determine the relative standard deviation of each ECL intensity, as shown in Fig. S19.

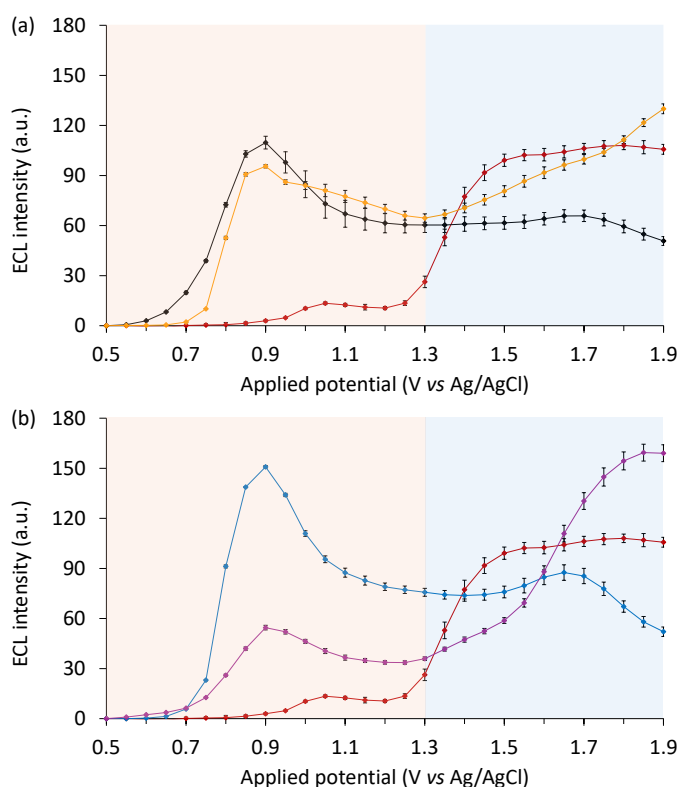


Figure S19. ECL intensity (integrated spectrum) across the potential range for (a, b) $10 \mu\text{M}$ $[\text{Ru}(\text{bpy})_3]^{2+}$ without a redox mediator (red plot), or with $100 \mu\text{M}$ redox mediator: (a) Ir(ppy)₃ (black plot) and Ir(ppy)₂(acac) (orange plot), or (b) Ir(ppz)₃ (blue plot) and Ir(pmi)₃ (purple plot), in acetonitrile containing 10 mM TPrA and 0.1 M TBAPF₆. Error bars show $\pm 1\sigma$ for three replicate experiments.

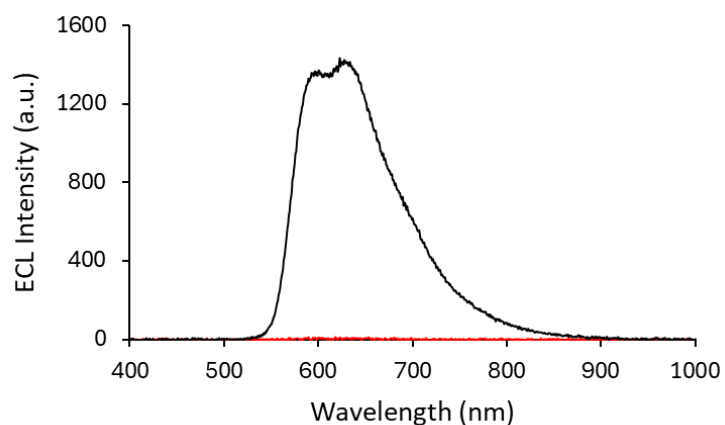


Figure S20. Mixed annihilation spectrum (black plot) of a mixture of $[\text{Ir}(\text{piq})_2(\text{dm-bpy})]^+$ ($10 \mu\text{M}$) and $\text{Ir}(\text{pmi})_3$ ($100 \mu\text{M}$), collected by alternating the applied potential (2.5 Hz for 2 s) between $-1.55 \text{ V vs Ag/AgCl}$ (to reduce $[\text{Ir}(\text{piq})_2(\text{dm-bpy})]^+$) and $0.77 \text{ V vs Ag/AgCl}$ (to oxidise $\text{Ir}(\text{pmi})_3$). The red plot shows the spectrum collected when applying the same potential pulse sequence in the absence of the redox mediator.

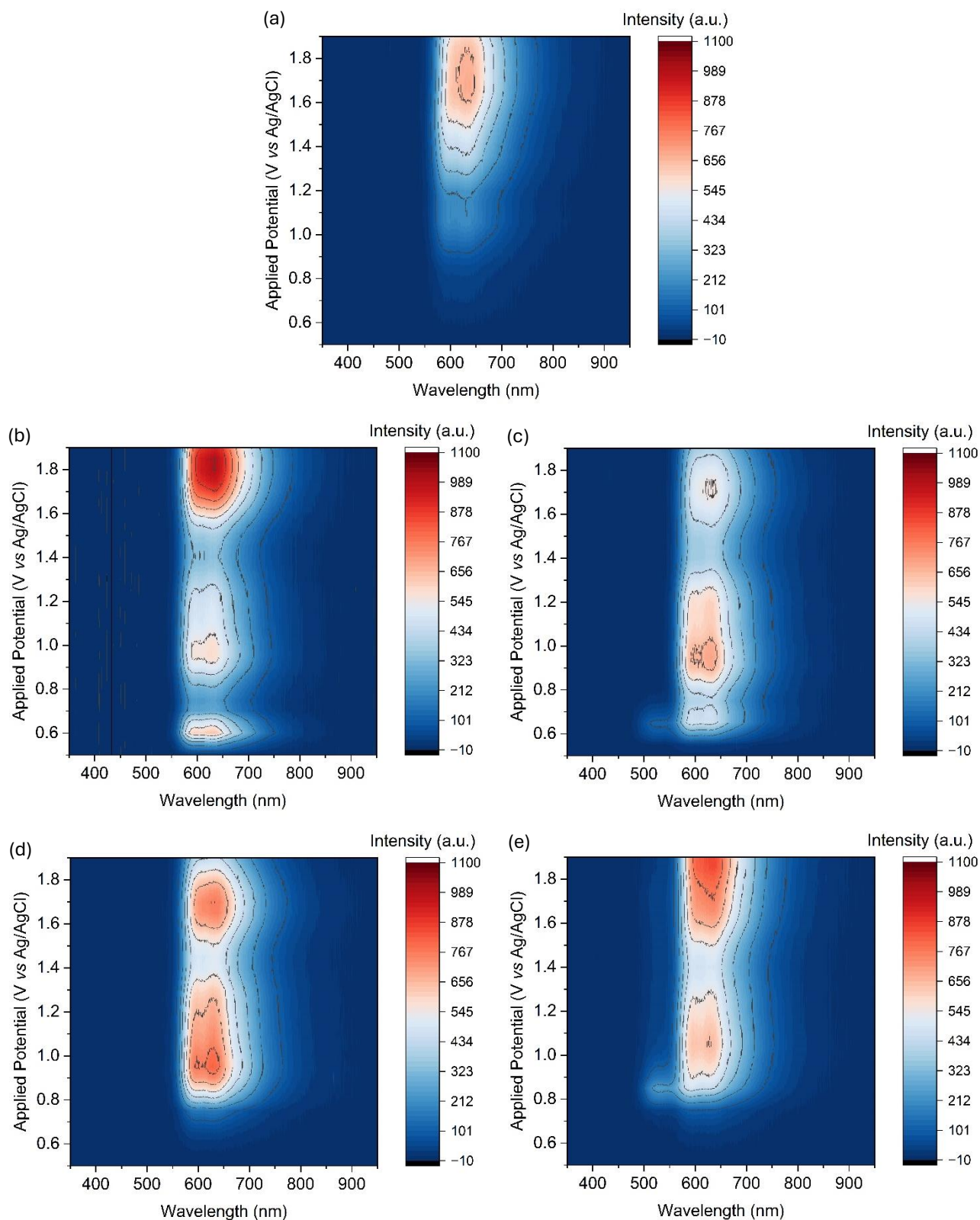


Figure S21. Contour plots of ECL intensity versus wavelength and applied potential for $[\text{Ir}(\text{pic})_2(\text{dm-bpy})]^+$ with (a) no redox mediator, (b) $\text{Ir}(\text{pmi})_3$, (c) $\text{Ir}(\text{ppy})_3$, (d) $\text{Ir}(\text{ppz})_3$, or (e) $\text{Ir}(\text{ppy})_2(\text{acac})$. Conditions: 10 μM luminophore and 100 μM redox mediator in acetonitrile containing 10 mM TPA as co-reactant and 0.1 M TBAPF_6 as supporting electrolyte.

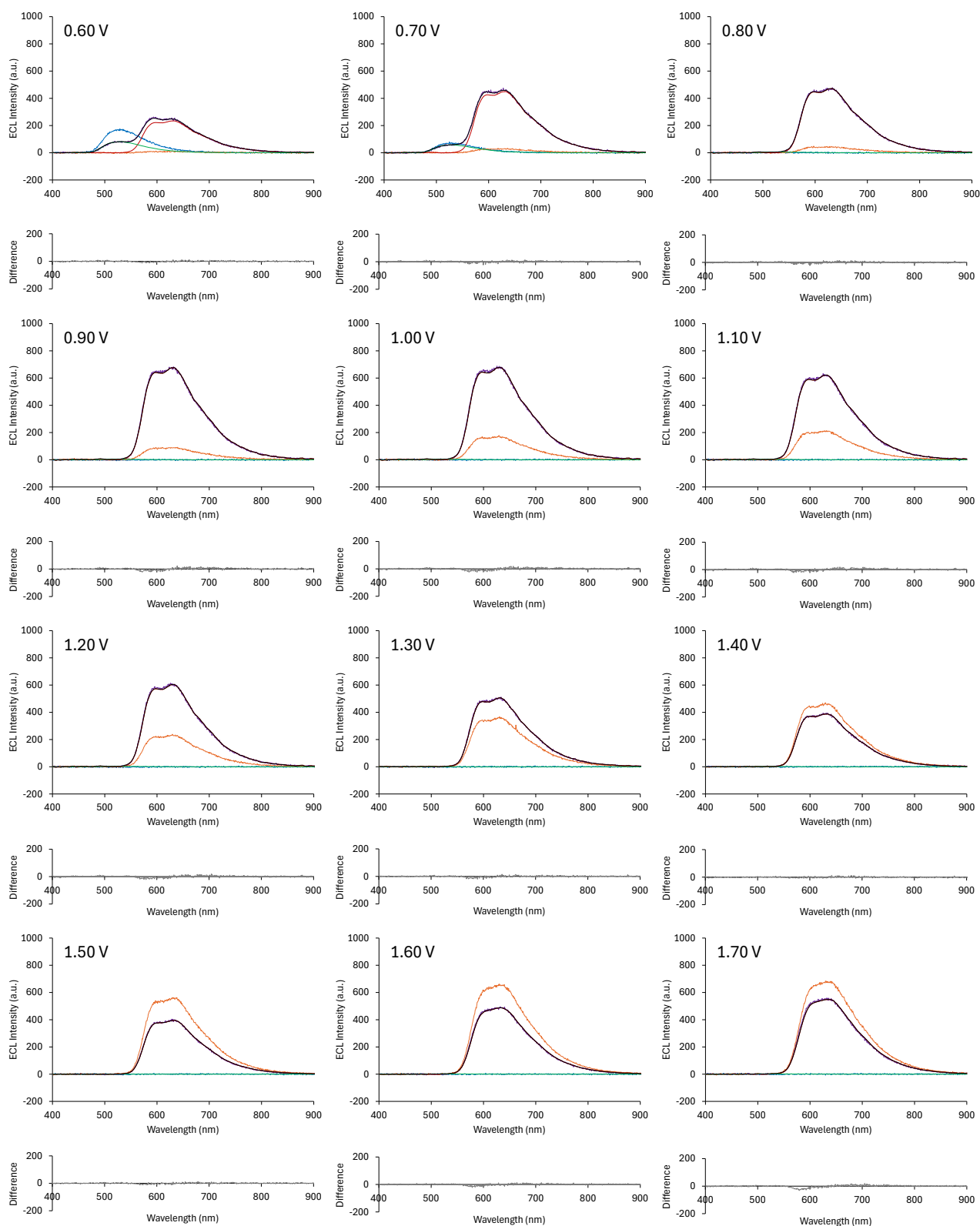


Figure S22. Selected spectra obtained from spooling ECL experiments for the $[\text{Ir}(\text{piq})_2(\text{dm-bpy})]^+$ luminophore (orange plot), $\text{Ir}(\text{ppy})_3$ mediator (blue plot), and a mixture of $[\text{Ir}(\text{piq})_2(\text{dm-bpy})]^+$ and $\text{Ir}(\text{ppy})_3$ (purple plot). The black plot shows the model spectrum of the mixture, which was deconvoluted into contributions from $[\text{Ir}(\text{piq})_2(\text{dm-bpy})]^+$ (red plot) and $\text{Ir}(\text{ppy})_3$ (green plot). The residuals for the modelled ECL spectrum are shown in the grey plot below. Experimental conditions: 10 μM luminophore and/or 100 μM redox mediator in acetonitrile containing 10 mM TPrA as co-reactant and 0.1 M TBAPF_6 as supporting electrolyte.

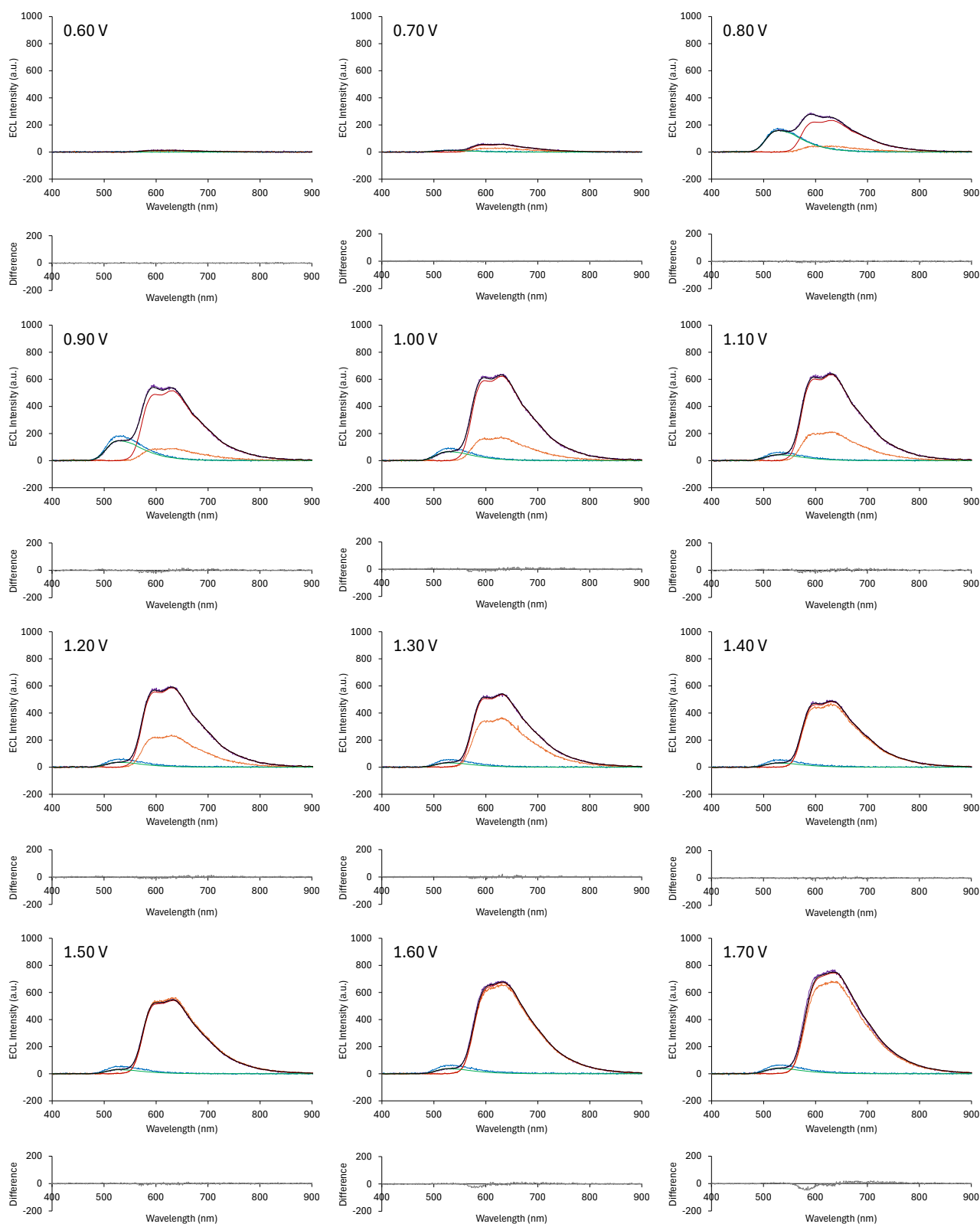


Figure S23. Selected spectra obtained from spooling ECL experiments for the $[\text{Ir}(\text{piq})_2(\text{dm-bpy})]^+$ luminophore (orange plot), $\text{Ir}(\text{ppy})_2(\text{acac})$ mediator (blue plot), and a mixture of $[\text{Ir}(\text{piq})_2(\text{dm-bpy})]^+$ and $\text{Ir}(\text{ppy})_2(\text{acac})$ (purple plot). The black plot shows the model spectrum of the mixture, which was deconvoluted into contributions from $[\text{Ir}(\text{piq})_2(\text{dm-bpy})]^+$ (red plot) and $\text{Ir}(\text{ppy})_2(\text{acac})$ (green plot). The residuals for the modelled ECL spectrum are shown in the grey plot below. Experimental conditions: 10 μM luminophore and/or 100 μM redox mediator in acetonitrile containing 10 mM TPrA as co-reactant and 0.1 M TBAPF_6 as supporting electrolyte.

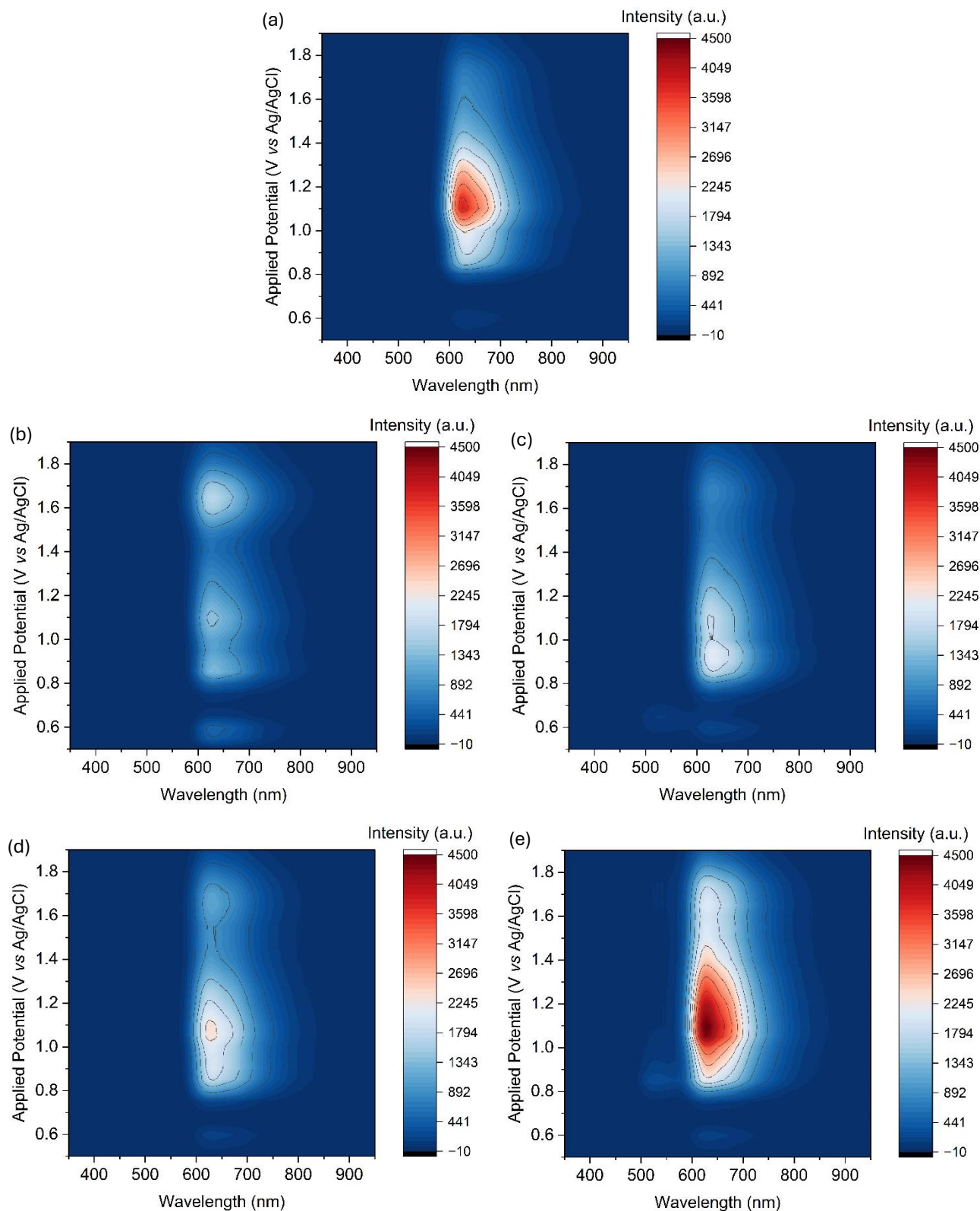


Figure S24. Contour plots of ECL intensity versus wavelength and applied potential for Ir(piq)₂(acac) with (a) no redox mediator, (b) Ir(pmi)₃, (c) Ir(ppy)₃, (d) Ir(ppz)₃, or (e) Ir(ppy)₂(acac). Conditions: 10 μ M luminophore and 100 μ M redox mediator in acetonitrile containing 10 mM TPrA as co-reactant and 0.1 M TBAPF₆ as supporting electrolyte.

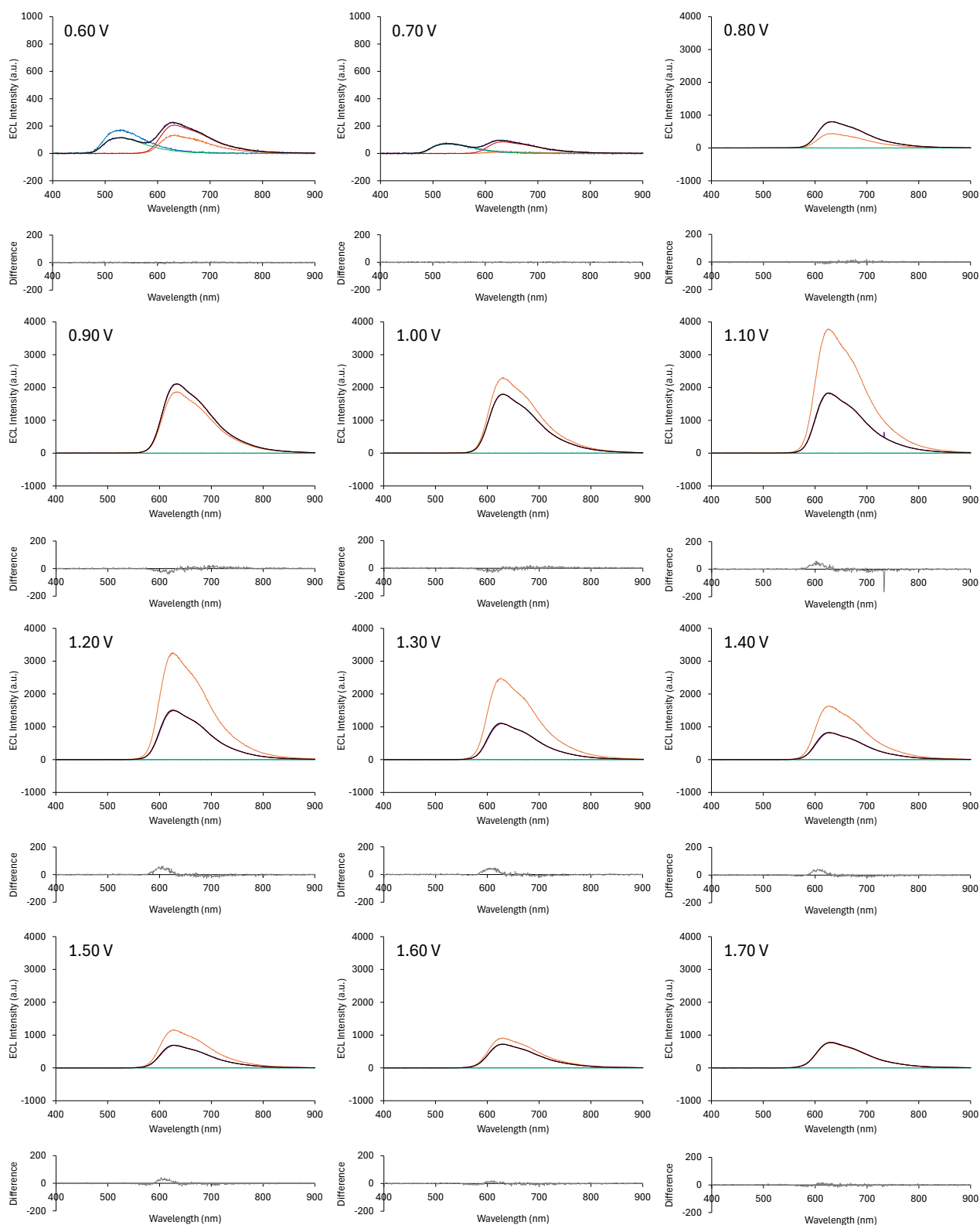


Figure S25. Selected spectra obtained from spooling ECL experiments for the Ir(piq)₂(acac) luminophore (orange plot), Ir(ppy)₃ mediator (blue plot), and a mixture of Ir(piq)₂(acac) and Ir(ppy)₃ (purple plot). The black plot shows the model spectrum of the mixture, which was deconvoluted into contributions from Ir(piq)₂(acac) (red plot) and Ir(ppy)₃ (green plot). The residuals for the modelled ECL spectrum are shown in the grey plot below. Experimental conditions: 10 μM luminophore and/or 100 μM redox mediator in acetonitrile containing 10 mM TPrA as co-reactant and 0.1 M TBAPF₆ as supporting electrolyte.

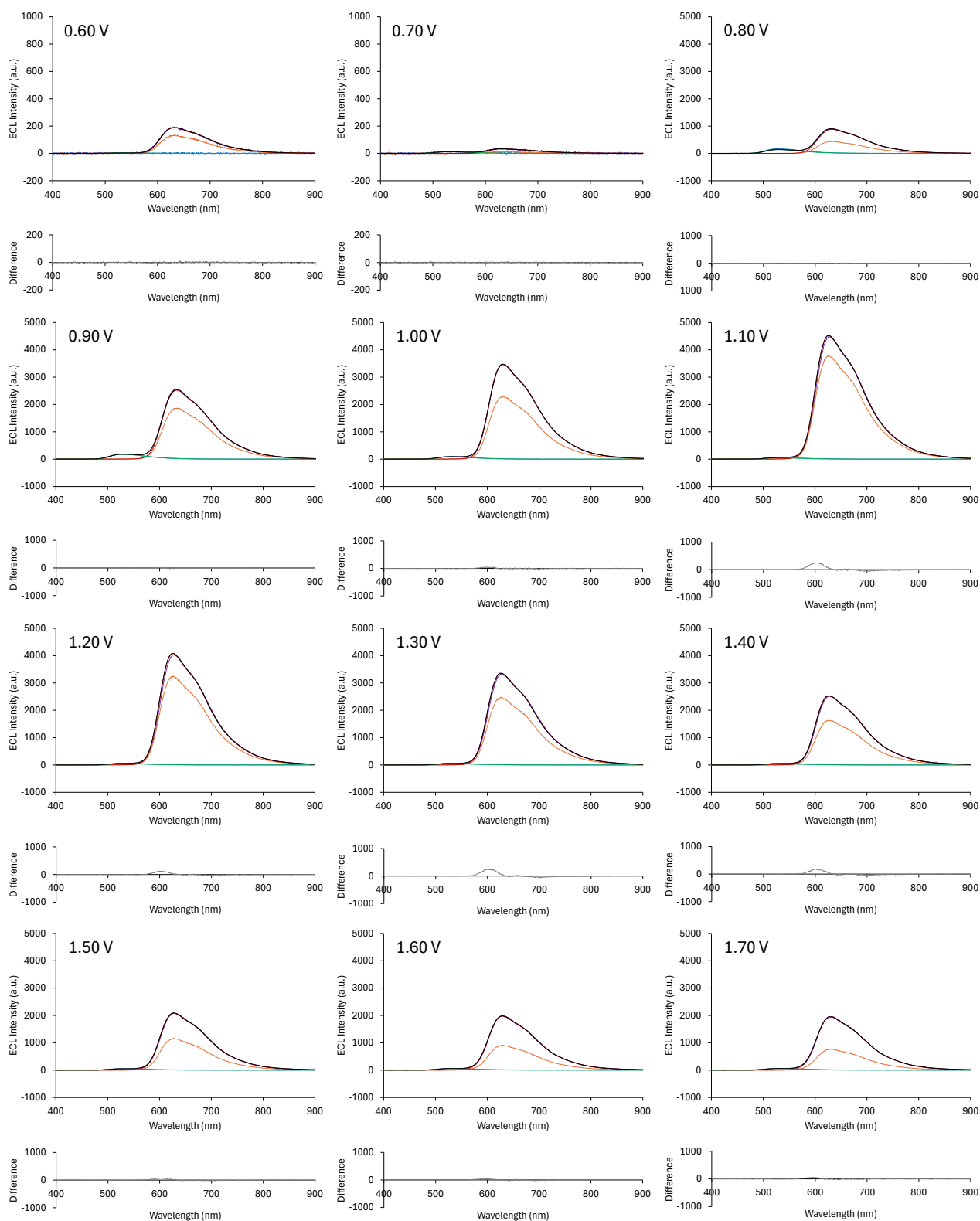


Figure S26. Selected spectra obtained from spooling ECL experiments for the Ir(piq)₂(acac) luminophore (orange plot), Ir(ppy)₂(acac) mediator (blue plot), and a mixture of Ir(piq)₂(acac) and Ir(ppy)₂(acac) (purple plot). The black plot shows the model spectrum of the mixture, which was deconvoluted into contributions from Ir(piq)₂(acac) (red plot) and Ir(ppy)₂(acac) (green plot). The residuals for the modelled ECL spectrum are shown in the grey plot below. Experimental conditions: 10 μM luminophore and/or 100 μM redox mediator in acetonitrile containing 10 mM TPrA as co-reactant and 0.1 M TBAPF₆ as supporting electrolyte.

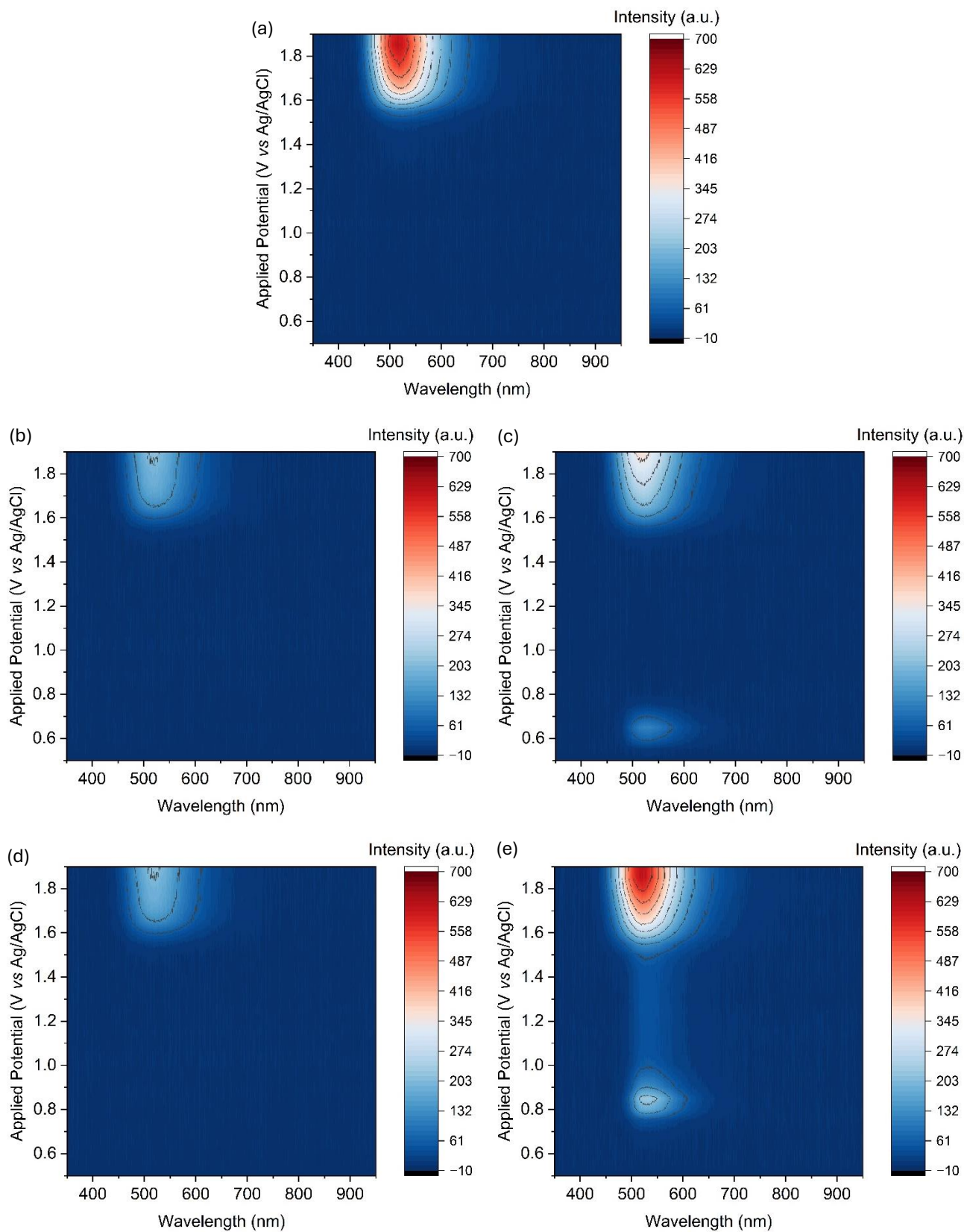


Figure S27. Contour plots of ECL intensity versus wavelength and applied potential for $[\text{Ir}(\text{df-ppy})_2(\text{dm-bpy})]^+$ with (a) no redox mediator, (b) $\text{Ir}(\text{pmi})_3$, (c) $\text{Ir}(\text{ppy})_3$, (d) $\text{Ir}(\text{ppz})_3$, or (e) $\text{Ir}(\text{ppy})_2(\text{acac})$. Conditions: 10 μM luminophore and 100 μM redox mediator in acetonitrile containing 10 mM TPrA as co-reactant and 0.1 M TBAPF₆ as supporting electrolyte.

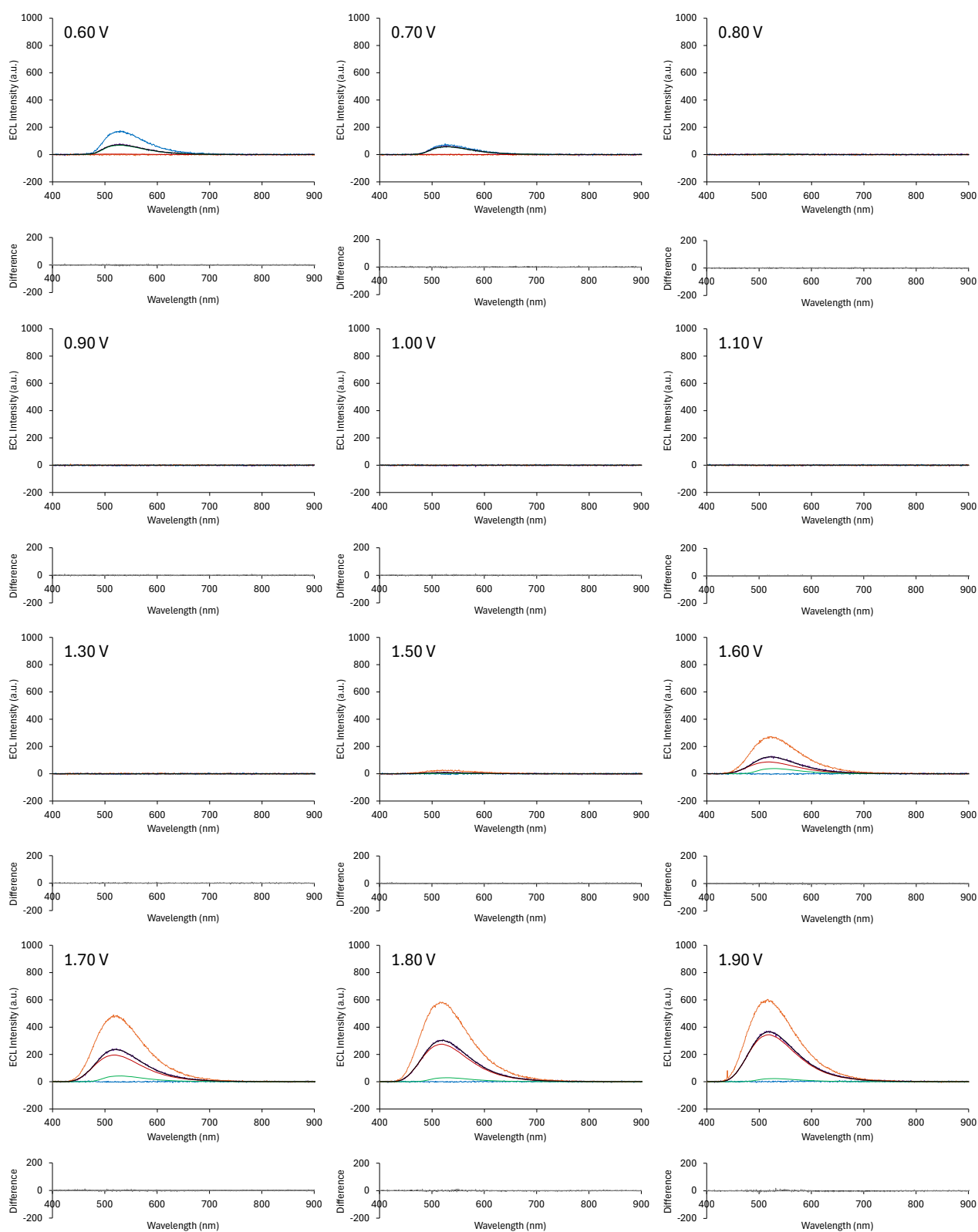


Figure S28. Selected spectra obtained from spooling ECL experiments for the $[\text{Ir}(\text{df-ppy})_2(\text{dm-bpy})]^+$ luminophore (orange plot), $\text{Ir}(\text{ppy})_3$ mediator (blue plot), and a mixture of $[\text{Ir}(\text{df-ppy})_2(\text{dm-bpy})]^+$ and $\text{Ir}(\text{ppy})_3$ (purple plot). The black plot shows the model spectrum of the mixture, which was deconvoluted into contributions from $[\text{Ir}(\text{df-ppy})_2(\text{dm-bpy})]^+$ (red plot) and $\text{Ir}(\text{ppy})_3$ (green plot). The residuals for the modelled ECL spectrum are shown in the grey plot below. Experimental conditions: 10 μM luminophore and/or 100 μM redox mediator in acetonitrile containing 10 mM TPrA as co-reactant and 0.1 M TBAPF_6 as supporting electrolyte.

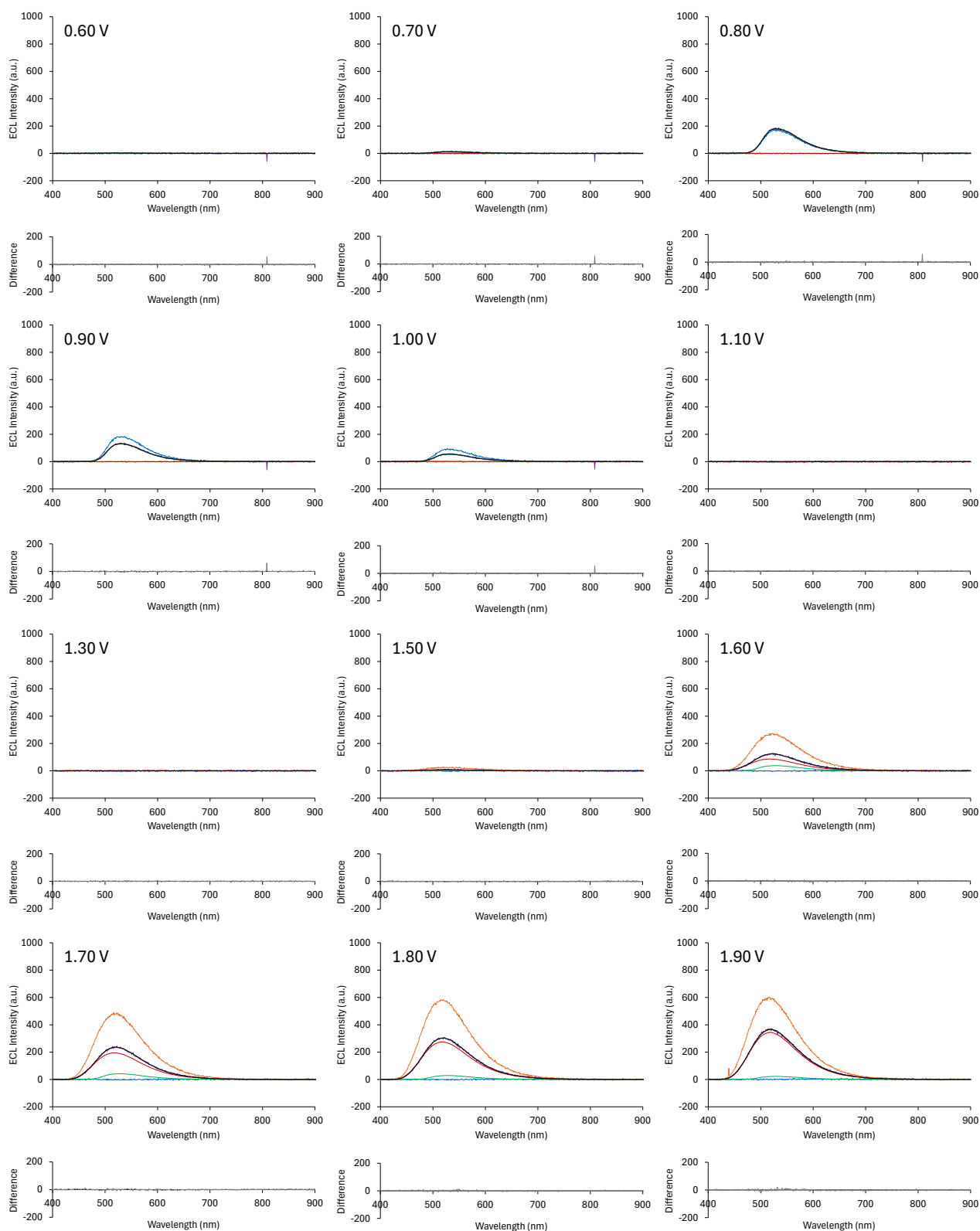


Figure S29. Selected spectra obtained from spooling ECL experiments for the $[\text{Ir}(\text{df-ppy})_2(\text{dm-bpy})]^+$ luminophore (orange plot), $\text{Ir}(\text{ppy})_2(\text{acac})$ mediator (blue plot), and a mixture of $[\text{Ir}(\text{df-ppy})_2(\text{dm-bpy})]^+$ and $\text{Ir}(\text{ppy})_2(\text{acac})$ (purple plot). The black plot shows the model spectrum of the mixture, which was deconvoluted into contributions from $[\text{Ir}(\text{df-ppy})_2(\text{dm-bpy})]^+$ (red plot) and $\text{Ir}(\text{ppy})_2(\text{acac})$ (green plot). The residuals for the modelled ECL spectrum are shown in the grey plot below. Experimental conditions: 10 μM luminophore and/or 100 μM redox mediator in acetonitrile containing 10 mM TPrA as co-reactant and 0.1 M TBAPF_6 as supporting electrolyte.